



Original Article

# Roles of SET7/9 and LSD1 in the Pathogenesis of Arsenic-induced Hepatocyte Apoptosis

Bing Han<sup>1,2#</sup>, Yi Yang<sup>1,2#</sup>, Lei Tang<sup>3#</sup>, Qin Yang<sup>1,2</sup> and Rujia Xie<sup>1,2\*</sup>

<sup>1</sup>Department of Pathophysiology, College of Basic Medical Sciences, Guizhou Medical University, Guiyang, Guizhou, China; <sup>2</sup>Guizhou Provincial Key Laboratory of Pathogenesis and Drug Research on Common Chronic Diseases, Guizhou Medical University, Guiyang, Guizhou, China; <sup>3</sup>Medical College of Guizhou University, Guiyang, Guizhou, China

Received: 28 December 2020 | Revised: 22 February 2021 | Accepted: 11 March 2021 | Published: 16 April 2021

## Abstract

**Background and Aims:** Multiple regulatory mechanisms play an important role in arsenic-induced liver injury. To investigate whether histone H3 lysine 4 (H3K4) methyltransferase (SET7/9) and histone H3K4 demethyltransferase (LSD1/KDM1A) can regulate endoplasmic reticulum stress (ERS)-related apoptosis by modulating the changes of H3K4 methylations in liver cells treated with arsenic. **Methods:** Apoptosis, proliferation and cell cycles were quantified by flow cytometry and real-time cell analyzer. The expression of ERS- and epigenetic-related proteins was detected by Western blot analysis. The antisense SET7/9 expression vector and the overexpressed LSD1 plasmid were used for transient transfection of LO2 cells. The effects of NaAsO<sub>2</sub> on the methylation of H3 in the promoter regions of 78 kDa glucose-regulated protein, activating transcription factor 4 and C/EBP-homologous protein were evaluated by chromatin immunoprecipitation assay. **Results:** The protein expression of LSD1 (1.25±0.08 vs. 1.77±0.08, *p*=0.02) was markedly decreased by treatment with 100 μM NaAsO<sub>2</sub>, whereas the SET7/9 (0.68±0.05 vs. 1.10±0.13, *p*=0.002) expression level was notably increased, which resulted in increased H3K4me1/2 (0.93±0.64, 1.19±0.22 vs. 0.71±0.13, 0.84±0.13, *p*=0.03 and *p*=0.003). After silencing SET7/9 and overexpressing LSD1 by transfection, apoptosis rate (in percentage: 3.26±0.34 vs. 7.04±0.42, 4.80±0.32 vs. 7.52±0.38, *p*=0.004 and *p*=0.02) was significantly decreased and proliferation rate was notably increased, which is reversed after inhibiting LSD1 (in percentage: 9.31±0.40 vs. 7.52±0.38, *p*=0.03). Furthermore, the methylation levels of H3 in the promoter regions of GRP78 (20.80±2.40 vs. 11.75±2.47, 20.46±2.23 vs. 14.37±0.91, *p*=0.03 and *p*=0.01) and CHOP (48.67±4.04

vs. 16.67±7.02, 59.33±4.51 vs. 20.67±3.06, *p*=0.004 and *p*=0.001) were significantly increased in LO<sub>2</sub> cells exposed to 100 μM NaAsO<sub>2</sub> for 24 h. **Conclusions:** Histone methyltransferase SET7/9 and histone demethyltransferase LSD1 jointly regulate the changes of H3K4me1/me2 levels in arsenic-induced apoptosis. NaAsO<sub>2</sub> induces apoptosis in LO2 cells by activating the ERS-mediated apoptotic signaling pathway, at least partially by enhancing the methylation of H3 on the promoter regions of ERS-associated genes, including GRP78 and CHOP.

**Citation of this article:** Han B, Yang Y, Tang L, Xie R, Yang Q. Roles of SET7/9 and LSD1 in the pathogenesis of arsenic-induced hepatocyte apoptosis. J Clin Transl Hepatol 2021;9(3):364–372. doi: 10.14218/JCTH.2020.00185.

## Introduction

Arsenic is a non-metal element, widely distributed in soil, water, minerals and plants in nature; and long-term exposure to a high-arsenic environment can cause arsenic poisoning in the organism.<sup>1–3</sup> A large number of epidemiological investigations and animal experiments have shown that arsenic poisoning can cause liver damage, and even lead to cirrhosis and liver cancer, which has become the main cause of death in patients with arsenic poisoning.<sup>4,5</sup> Therefore, there is an urgent need to identify novel therapeutic targets and to develop effective strategies for liver damage therapy. At present, studies on the mechanism of liver injury caused by arsenic poisoning mainly focus on oxidative stress,<sup>6</sup> influence on enzyme activity,<sup>7</sup> DNA damage, DNA methylation,<sup>8</sup> and apoptosis.<sup>9,10</sup> Observations of involvement of many various mechanisms indicate that arsenic-induced hepatocyte apoptosis is one of the core events.<sup>11,12</sup>

Arsenic can upregulate the expression levels of Fas and Fas ligand (i.e. FasL) in liver cells, and increase the apoptosis of cells through the death receptor pathway, causing liver damage.<sup>13,14</sup> Some scholars have found that arsenic can increase the expression levels of Bax and p53 proteins and induce hepatocyte apoptosis through a mitochondrial pathway.<sup>15,16</sup> While the endoplasmic reticulum (ER) is physiologically responsible for the control of proper protein folding and function, many factors such as the unfolded protein response, ER overload response and others, can disturb ER function, leading to ER stress (ERS). Apoptosis induced by ERS is a newly-discovered apoptosis pathway

**Keywords:** Arsenic; SET7/9; LSD1; H3K4me1/2; ER stress.

**Abbreviations:** AI, artificial intelligence; ATF4, activating transcription factor 4; ChIP, chromatin immunoprecipitation assay; CHOP, C/EBP-homologous protein; EDTA, ethylene diamine tetraacetic acid; ER, endoplasmic reticulum; ERS, endoplasmic reticulum stress; GRP78, 78 kDa glucose-regulated protein; H3K4, histone 3 lysine 4; LSD1/KDM1A, histone 3 lysine 4 demethyltransferase; me, methylation; PBS, phosphate-buffered saline; PERK, PRKR-like endoplasmic reticulum kinase; RTCA, real-time cell analyzer; RUCAM, Roussel Uclaf causality assessment method; SET7/9, histone 3 lysine 4 methyltransferase; shRNA, small hairpin; siRNA, small interfering RNA.

#These authors contributed equally to this study.

\*Correspondence to: Rujia Xie, Department of Pathophysiology, College of Basic Medical Sciences, Guizhou Medical University, Guiyang, Guizhou 550000, China. ORCID: <https://orcid.org/0000-0001-5991-2678>. Tel: +86-13985441220, E-mail: 592153968@qq.com

following the death receptor pathway and the mitochondrial pathway.<sup>17,18</sup> Previous studies have also demonstrated ERS-mediated hepatocyte apoptosis in rats.<sup>19</sup> Further study found the PRKR-like endoplasmic reticulum kinase (PERK) signaling pathway were activated in arsenic-mediated liver cells.<sup>20</sup>

However, how the PERK signaling pathway is activated has not been deeply researched. In recent years, epigenetics has gradually become a research hotspot. Epigenetics is a branch of genetics that studies the heritable changes in gene expression without changes in nucleotide sequence. Some scholars have found that the expression levels of 78 kDa glucose-regulated protein (GRP78), histone 3 lysine 4 methyltransferase (SET7/9) and histone 3 lysine 4 (H3K4) me2 are significantly increased in the renal tissues of diabetic nephrotic mice,<sup>21</sup> suggesting that epigenetic histone modification may be associated with ERS. SET/9 specifically monomethylates the fourth lysine of histone 3 (i.e. H3K4) in multiple modifiable sites of histones.<sup>22,23</sup> Studies have shown that sodium arsenite can upregulate the level of dimethyl and methyl modification of H3K4 by downregulating the expression level of LSD1, which can open or increase the transcription of some genes.<sup>24</sup> Lysine-specific histone demethylase 1 (LSD1, also known as KDM1A), is a member of the amine oxidase family and a member of the demethylase family. LSD1 serves as a demethylase that specifically removes dimethyl and methyl modifications of H3K4 *in vitro*.

Based on the above research background, this experiment was designed to investigate whether SET7/9 and LSD1/KDM1A can regulate ERS-related apoptosis by modulating the changes of H3K4 methylations in liver cells treated with arsenic.

## Methods

### Cells and reagents

Human normal hepatocyte LO2 cells were obtained from the Shanghai Cell Bank of Chinese Academy of Sciences (China) and sodium arsenite was obtained from Shandong Xiya Reagent Chemical Industry (China). Fetal bovine serum, Dulbecco's modified Eagle's medium (GIBCO, New York, NY, USA), antibodies against GRP78, C/EBP-homologous protein (CHOP), LSD1, H3 and H3K4me1 (Abcam, Cambridge, UK), antibodies against H3K4me2 (Active Motif, Carlsbad, CA, USA), GAPDH (Bioprimacy Biotechnology, Wuhan, China), secondary antibodies (Boster Biological Engineering, Wuhan, China), SET7/9-specific small interfering RNAs (siRNAs) were purchased from Shanghai Jima Gene (China), negative small hairpin (sh)RNA and LSD1 overexpressed plasmids were obtained from Shanghai Jima Gene. OG-L002, an effective and selective LSD1 inhibitor, was obtained from Selleck Chemicals Company (Houston, USA). The chromatin immunoprecipitation assay (ChIP) kit and Lipofectamine 2000 were procured from Thermo Fisher Scientific (Waltham, MA, USA). The cell cycle and apoptosis detection kit were purchased from Bormai Biotechnology (Beijing, China)

### Real-time cellular analysis

Cell proliferation was monitored using an xCELLigence Real-Time Cell Analysis instrument (xCELLigence DP System; ACEA Biosciences, Inc., San Diego, CA, USA), which can continuously monitor live cell proliferation, morphology and viability with a label-free assay. A 100  $\mu$ L aliquot of LO2 sus-

pended droplets were added to an E-Plate, including 10,000 cells, which was placed at 37°C in a humidified incubator containing 5% CO<sub>2</sub> for 6–8 h. After LO2 cells adhered to the plate, arsenic was added at 100  $\mu$ M,<sup>20</sup> and we performed continuous monitoring of the cell growth and proliferation process for 36 to 48 h.

### Western blot

Taking out each cell culture, and adding "protein lysis solution" and protease inhibitors at a ratio of 99:1, each cell suspension was collected into a 1.5 mL centrifuge tube after lysing on the ice for 10 m; then, the 1.5 mL centrifuge tubes were centrifuged at 4°C and 12,000 r/m for 20 m. After precipitating, collecting the supernatant, and transferring the proteins to PVDF membranes, non-specific binding was blocked with 5% non-fat dry milk in Tris-buffered saline with Tween-20, and the membranes were probed overnight at 4°C with primary antibodies against GRP78 (1:1,500), CHOP (1:1,500), GAPDH (1:1,000), H3 (1:1,000), H3K4me1 (1:1,000), and H3K4me2 (1:1,000). The bound antibodies were detected with horseradish peroxidase-conjugated secondary antibodies and visualized using enhanced chemiluminescence reagents. The signal intensity was measured using Bio-Rad imaging system (Hercules, CA, USA) and analyzed by Quantity One software (Bio-Rad).

### Apoptosis assay

Cells were digested with 0.25% trypsin without ethylene diamine tetraacetic acid (commonly referred to as EDTA) and washed with phosphate-buffered saline (PBS) 2–3 times; then, suspension liquids were collected into 10 mL centrifuge tubes. After centrifugation at 1,500 r/m for 5 m, 500  $\mu$ L of binding buffer was added into tubes and resuspended. Annexin V-FITC (5  $\mu$ L) and propidium iodide staining solution (5  $\mu$ L) were added for a 5–15 m incubation.

### Cell cycle assay

After the supernatant of each group was discarded and washed with PBS for 2–3 times, the cells of each group were digested with trypsin, free of EDTA, and the cell suspension was collected. The supernatant was discarded after centrifugation at 2,000 r/m for 5 m, and then washed with PBS to repeat the above steps. After the supernatant of the centrifuged tube was discarded, 250  $\mu$ L PBS was added for resuspending, and 750  $\mu$ L precooled anhydrous ethanol was added to each group to make the final concentration of ethanol 75%; after resuspension, the cells were incubated overnight at 4°C. On the second day, the cell suspensions of each group were centrifuged at 2,000 r/m for 5 m, and the supernatant was discarded. Then, the supernatant was processed with PBS in the same way. After the supernatant was discarded, the mixture of 500  $\mu$ L was configured for each group in the proportion of RNase: Propidium Iodide=1:9.

### ChIP-qPCR

LO2 cells ( $1 \times 10^6$ ) were seeded onto 10-cm diameter dishes and were mock-treated with PBS (0  $\mu$ mol/L NaAsO<sub>2</sub>) or 100  $\mu$ mol/L NaAsO<sub>2</sub> for 24 h. After treatment, ChIP kit (purchased from Thermo Fisher Scientific) was used to perform

**Table 1. DNA sequences of primers used for reverse transcription- and ChIP-quantitative PCR**

Gene	Forward, 5'-3'	Reverse, 5'-3'
GRP78	GGGATGGAGGAAGGGAGAAC	GAGGCATTTCCTGCTGTAAC
ATF4	GGTGGGTTCCATGGTCAAAT	AACACATCCACCACTGC
CHOP	CACGACCTCAGCCTGTCAAG	ACTGGAGTGGTGTGGCAATG

a ChIP assay. According to the manufacturer's instructions, LO2 cells were cross-linked with 16% formaldehyde, and 1× glycine was added to terminate the cross-linking. The cells were lysed with 2 μL cell nuclease (ChIP grade) lysis buffer and the lysates were ultrasound-crushed to a length of 150–1,000 bp. Immunoprecipitation was performed at 4°C for overnight using magnetic beads A/G and the following antibodies: rabbit IgG (1:10), anti-RNA polymerase II (1:10), anti-H3K4me1 (1:10), and anti-H3K4me2 (1:10). The immunoprecipitates were washed and eluted using magnetic scaffolding (purchased from Thermo Fisher Scientific). Immunoprecipitated DNA was recovered by reverse cross-linking, then purified and dissolved in distilled water. The corresponding sample without any antibody added served as input control. Objective DNA and input DNA were analyzed by reverse transcription-qPCR. The abundance of immunoprecipitated target DNA was expressed as the percentage of input chromatin DNA. The primer sequences of the target genes GRP78, activating transcription factor 4 (ATF4), and CHOP are listed in Table 1.

### Statistical analysis

SPSS 20.0 statistical software was used for analysis. Data were expressed as the mean±standard deviation. The one-way analysis of variance method was used for the multivariate comparison, and the least significant difference method was used as a post hoc test. A *p*-value of <0.05 was considered to indicate a statistically significant difference.

### Results

#### Arsenic significantly upregulates ERS-related proteins and H3K4me1/me2 in L02 cells

Compared with control group, the levels of SET7/9,<sup>20</sup> CHOP and H3K4me1 were significantly increased (Fig. 1B and Fig. 2B), whereas the level of LSD1 was obviously decreased

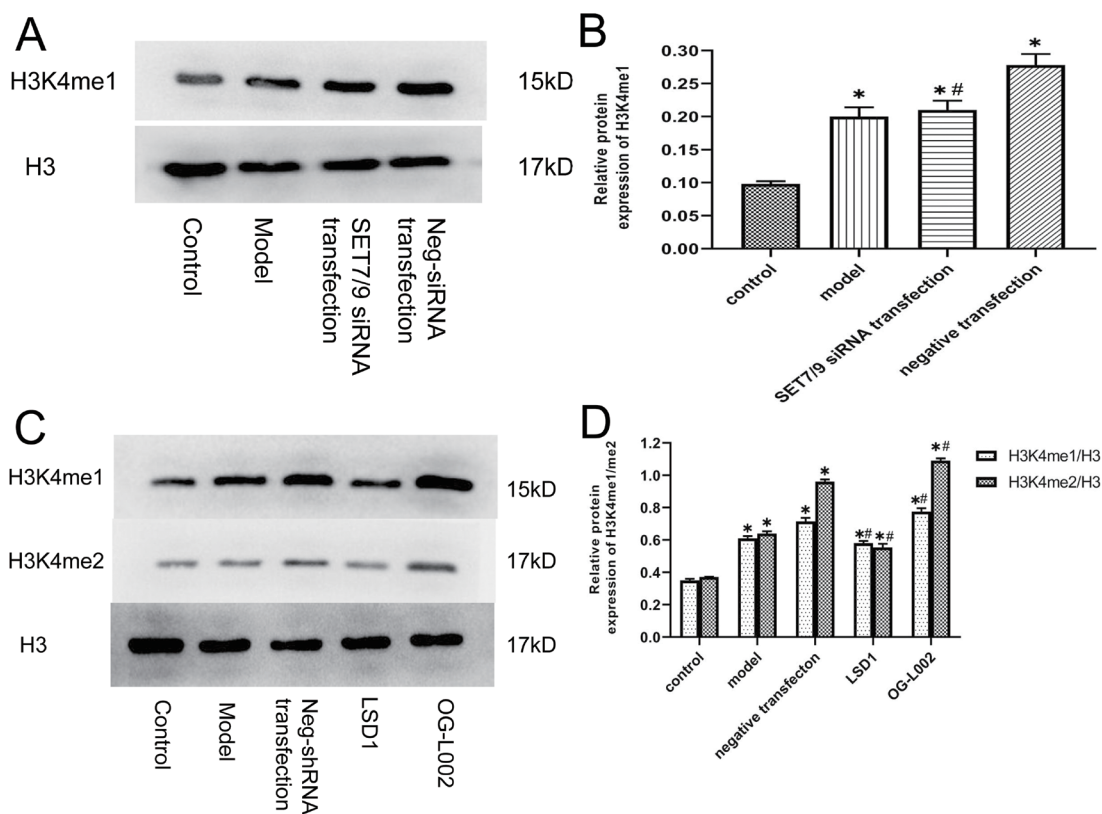


**Fig. 1. Effect of arsenic on H3K4 methylation in L02 hepatocytes.** Cells were exposed to arsenic at 100 μmol/L for 24 h. Proteins, prepared from whole cell extracts, were analyzed by western blotting. The activities of H3K4me1/me2 were determined with respective specific antibodies. (A) SET7/9 protein knock-down efficiency. H3K4me1 expression was measured in control, model and SET7/9 knock-down L02 cells. (B) Data shown are mean±standard deviation of three independent experiments, \**p*<0.05 vs. control group; #*p*<0.05 vs. negative transfection group. (C) LSD1 protein knock-down and overexpression efficiency. H3K4me1/me2 expression was measured in control, model and LSD1 knock-down and overexpression efficiency. (D) Data shown are mean±standard deviation of three independent experiments, \**p*<0.05 vs. control group; #*p*<0.05 vs. negative transfection group.

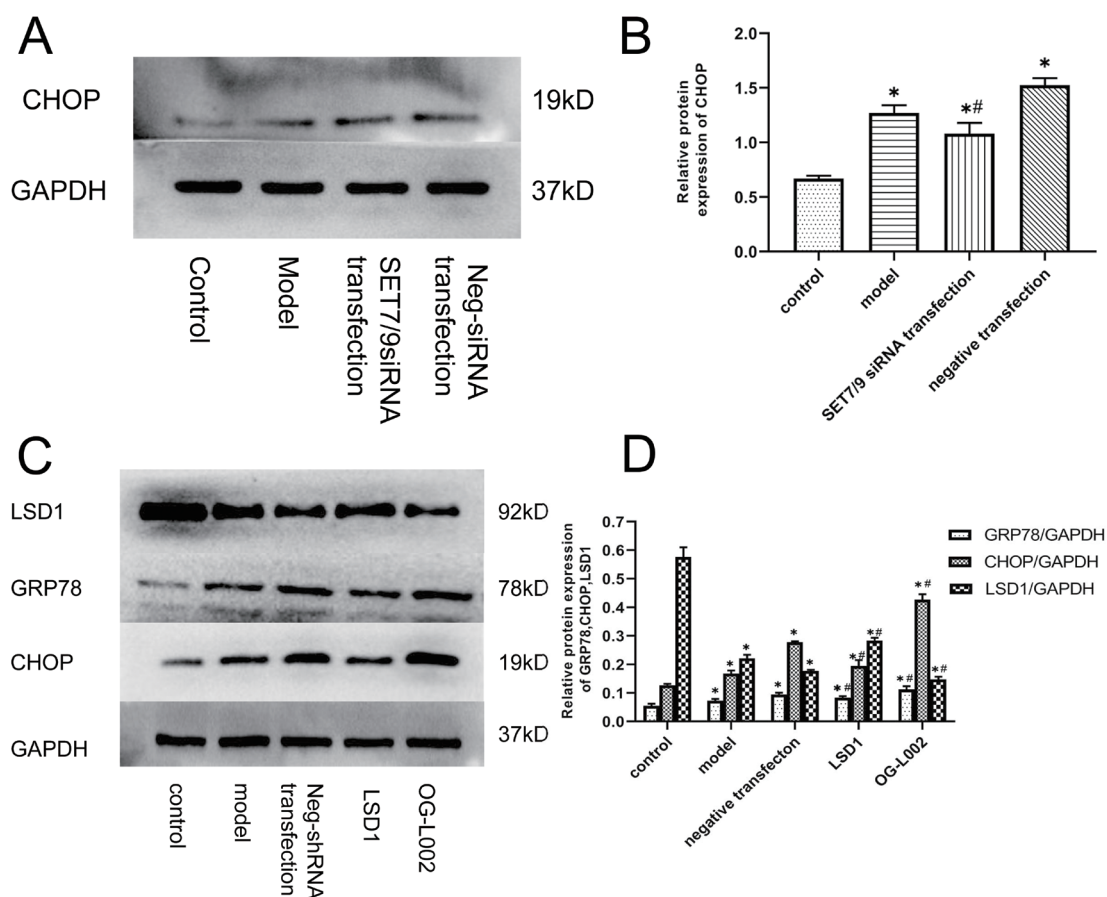


**Fig. 2. Effect of arsenic on ERS-related proteins in L02 hepatocytes.** Cells were exposed to arsenic at 100  $\mu\text{mol/L}$  for 24 h. Proteins, prepared from whole cell extracts, were analyzed by western blotting. The activities of GRP78, CHOP, and LSD1 were determined with respective specific antibodies. (A) SET7/9 protein knock-down efficiency. CHOP expression was measured in control, model and SET7/9 knock-down in L02 cells. (B) Data shown are mean $\pm$ standard deviation of three independent experiments, \* $p$ <0.05 vs. control group; # $p$ <0.05 vs. negative transfection group. (C) LSD1 protein knock-down and overexpression efficiency. GRP78, CHOP, and LSD1 expression was measured in control, model and LSD1 knock-down and OG-L002 group of L02 cells. (D) Data shown are mean $\pm$ standard deviation of three independent experiments, \* $p$ <0.05 vs. control group; # $p$ <0.05 vs. negative transfection group.

in the model group (Fig. 2D). Compared with the negative siRNA transfection group, the expression levels of GRP78, CHOP, and H3K4me1 in the SET7/9 siRNA transfection group (Fig. 1B and Fig. 2B) were significantly decreased.

Compared with the negative shRNA transfection group, the expression levels of GRP78, CHOP, H3K4me1, and H3K4me2 were significantly decreased in the LSD1 group (Fig. 1D and Fig. 2D); the expression levels of GRP78, CHOP, H3K4me1 and H3K4me2 were notably increased in the OG-L002 group (Fig. 1D and Fig. 2D).

**SET7/9 and LSD1 induce changes in apoptosis and cell cycle in L02 hepatocytes treated with arsenic**

Flow cytometry showed that the apoptosis rate and the proportion of G1 phase cells were significantly increased in the model group compared with the control group. Compared with the negative transfection group, the apoptosis rate and the proportion of G1 phase cells were notably decreased in the SET7/9 siRNA transfection group and the LSD1 overexpression group, while the apoptosis rate and the proportion of G1 phase cells were obviously increased in the OG-L002 group [Fig. 3A(f)]. These results indicate that arsenic could promote apoptosis and increase the proportion of G1 phase

cells, and histone modifying enzyme of SET7/9 and LSD1 could regulate apoptosis and cycle in arsenic-induced L02 cells [Fig. 3B(b) and 3C(b)]. The apoptotic data on SET7/9 has been published.<sup>20</sup>

**SET7/9 and LSD1 mediate proliferation changes in arsenic-induced L02 hepatocytes**

Real-time cellular analysis showed that the proliferation was significantly decreased in the model group compared with the control group. The proliferation rate was notably increased in the SET7/9 siRNA transfection group and in the LSD1 overexpression group compared with the negative transfection group, while the proliferation was obviously decreased in the OG-L002 group (Fig. 4B and 4D). These results illustrate that the histone modifying enzymes of SET7/9 and LSD1 could regulate proliferation in L02 cells.

**Arsenic treatment enhances the methylation level of histone H3 in the promoter regions of the GRP78 and CHOP genes in L02 hepatocytes**

In order to confirm whether the regulation of transcription

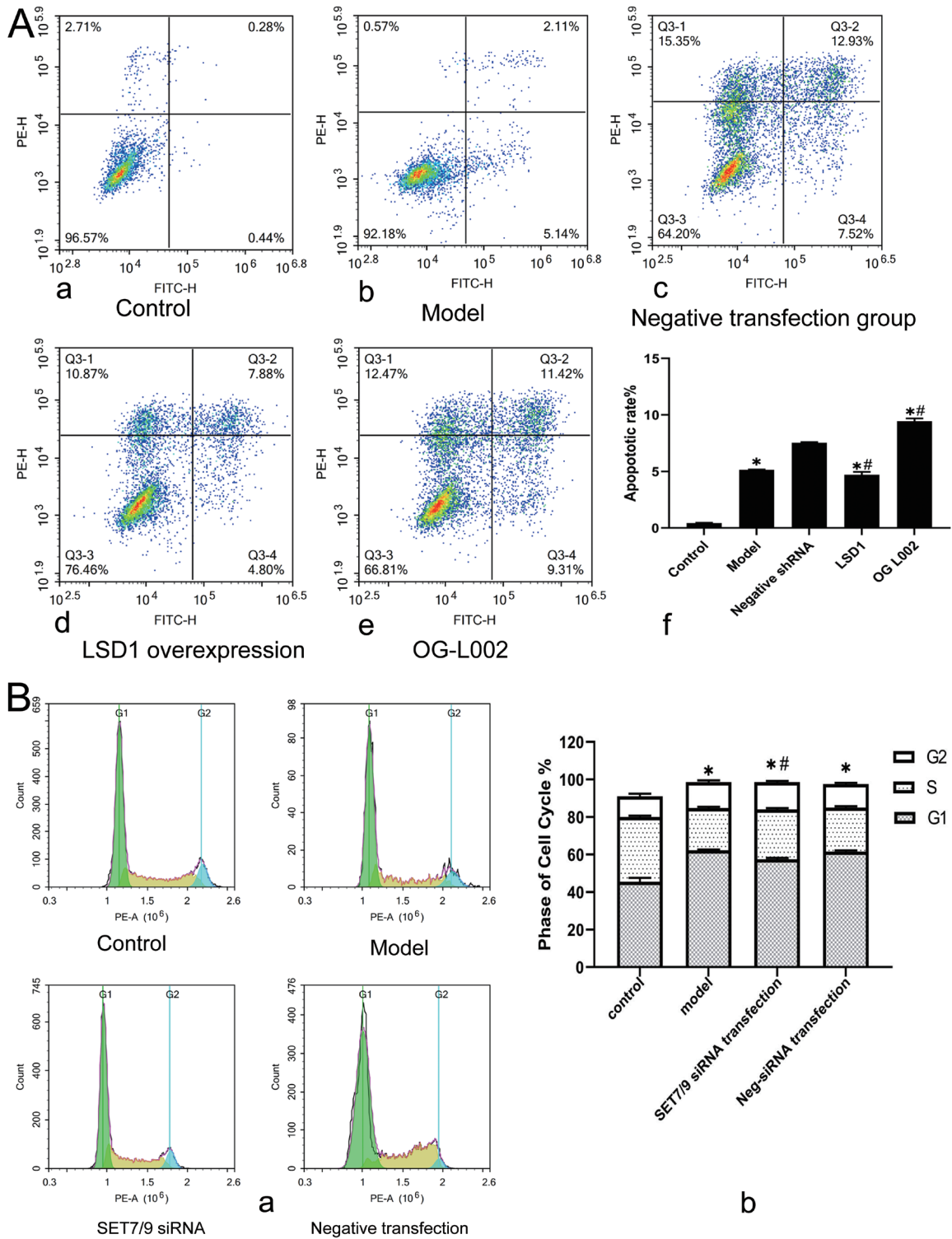
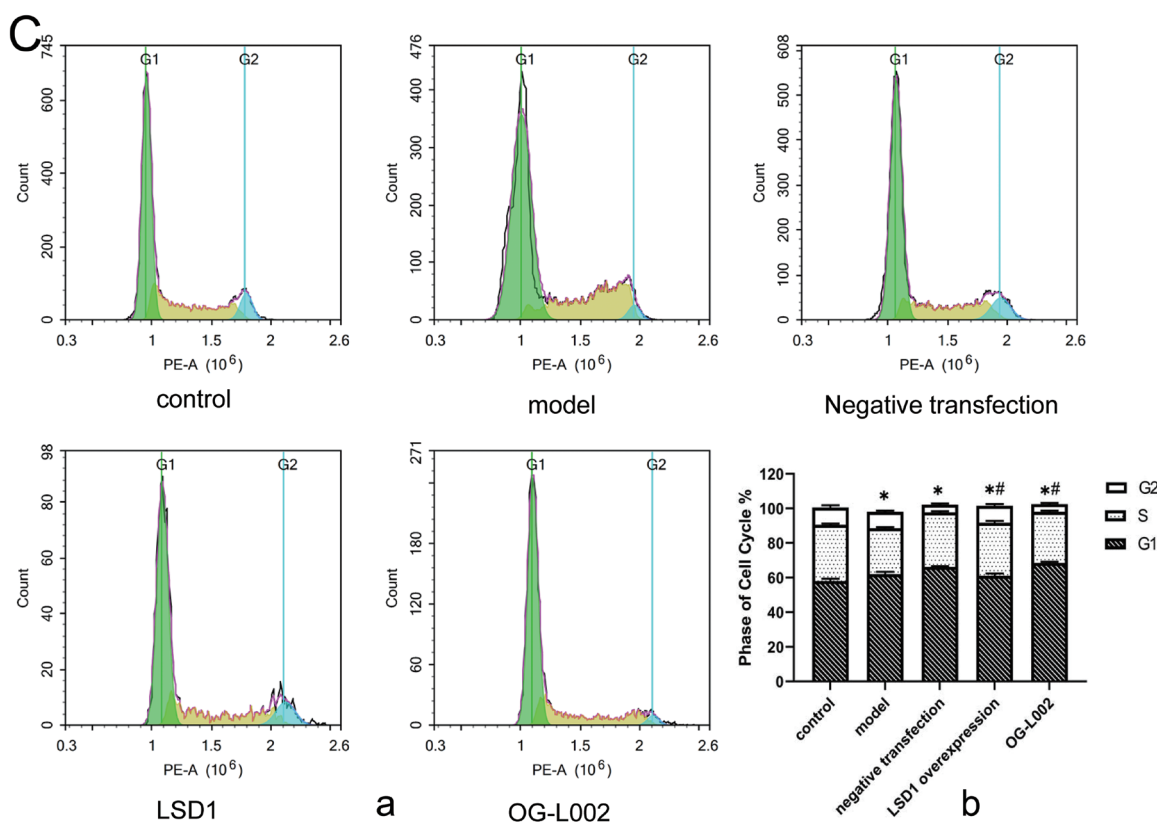


**Fig. 3. Effect of arsenic on apoptosis and cycles in L02 hepatocytes.** (A) The changes of apoptosis in the L02 cells of different groups were analyzed by flow cytometry. LSD1 protein knock-down and overexpression efficiency. Apoptosis was measured in control, model and LSD1 knock-down and OG-L002 group of L02 cells. (a: control; b: model; c: negative transfection; d: LSD1 overexpression group; e: OG-L002; f: the apoptosis rate of different groups) Data shown are mean±standard deviation of three independent experiments, \* $p < 0.05$  vs. control group; # $p < 0.05$  vs. negative transfection group. (B) The cell cycle distribution of each group. SET7/9 protein knock-down efficiency. Cell cycles were assessed in control, model and SET7/9 knock-down of L02 cells. (a: cycles diagram for each group; f: the cycles of different groups) Data shown are mean±standard deviation of three independent experiments, \* $p < 0.05$  vs. control group; # $p < 0.05$  vs. negative transfection group. (C) The cell cycle distribution of each group. Cycles were assessed in control, model and LSD1 knock-down and OG-L002 group of L02 cells. (a: cycles diagram for each group; f: the cycles of different groups) Data shown are mean±standard deviation of three independent experiments, \* $p < 0.05$  vs. control group; # $p < 0.05$  vs. negative transfection group.

Fig. 3. (continued)



of GRP78, ATF4 and CHOP genes by arsenic is mediated by the upregulation of H3K4me1/me2, ChIP was performed. Following treatment with arsenic, the L02 cells were lysed and immunoprecipitated with specific anti-H3K4me1/me2 antibody. qPCR results demonstrated a significant increase in the H3K4me1/me2-associated promoter regions of the GRP78 and CHOP genes in L02 cells treated with 100  $\mu$ M NaAsO<sub>2</sub> (Fig. 5A and 5C), while the promoter region of ATF4 did not show a significant increase in H3K4me1/me2 (Fig. 5B). These results confirmed that arsenic induces the expression of ERS-associated molecules by increasing their transcription, at least partially through enhancing the methylation of histone H3 in the promoter regions of these genes.

### Discussion

Arsenic can cause injury to many organs of the body,<sup>25</sup> among which liver injury has always been the focus.<sup>26,27</sup> In addition to endemic arsenic poisoning, medicine-induced arsenic poisoning also occurs.<sup>28</sup> Since ancient times, raw plants as well as refined plant products have been in common use, including as traditional Chinese medicine, Ayurveda in India, Kampo in Japan, traditional Korean medicine, and Unani in old Greece, all of which have well known associations with increased risk of liver damage.<sup>29</sup> In many countries, rice grains and complementary medicines are important sources of arsenic consumption.<sup>30</sup> Ayurvedic is an arsenic-containing compound, which is currently in use in India to control blood counts of patients with hematological malignancies.<sup>31</sup> Long-term use of the Ayurvedic drug can also cause liver damage.<sup>32</sup>

The Roussel Uclaf Causality Assessment Method (com-

monly known as RUCAM) is the best way to assess cause and effect in liver damage caused by arsenic poisoning from herbs and drugs. RUCAM, in its original version (published in 1993)<sup>33</sup> and its updated version (from 2016),<sup>34</sup> represents sophisticated diagnostic algorithms based on principles of artificial intelligence (commonly referred to as AI), as outlined in a recent editorial.<sup>35</sup>

At present, a clinical study of arsenic detoxification *in vivo* is under way. The arsenic detoxification treatment with dimercaptopropanol and sodium dimercaptopropanesulfonate has not achieved the expected efficacy in patients. The antagonistic effect of selenium on arsenic, the antioxidant effect of superoxide dismutase on patients with arsenic poisoning and the protective effect on liver, lung, kidney, heart and other organs have been widely reported in treatment studies. Guizhou province reports of Chinese herbal medicine preparation for the treatment of chronic arsenic poisoning causing liver damage, such as Lu *et al.*<sup>36</sup> showing that whether by clinical manifestations or through the preparation before and after the organizational structure of the liver samples of vivisection, compound preparation of the Chinese herbal medicine HanDan diisopropylamine dichloroacetate liver damage caused by arsenic poisoning still produces obvious curative effect. Yun *et al.*<sup>37</sup> used ginkgo biloba leaves to treat 84 cases of chronic arsenic poisoning caused by coal burning, with anti-liver fibrosis intent. Serology and pathological histology observations indicated that the serum platelet activation factor (an important factor involved in liver injury and fibrosis) and four liver fibrosis indexes in the treatment group were significantly decreased ( $p < 0.01$ ), and the liver pathology was also improved to a certain extent in the treatment group, which was statistically significant when compared with the non-ginkgo biloba control group ( $p > 0.01$ ).

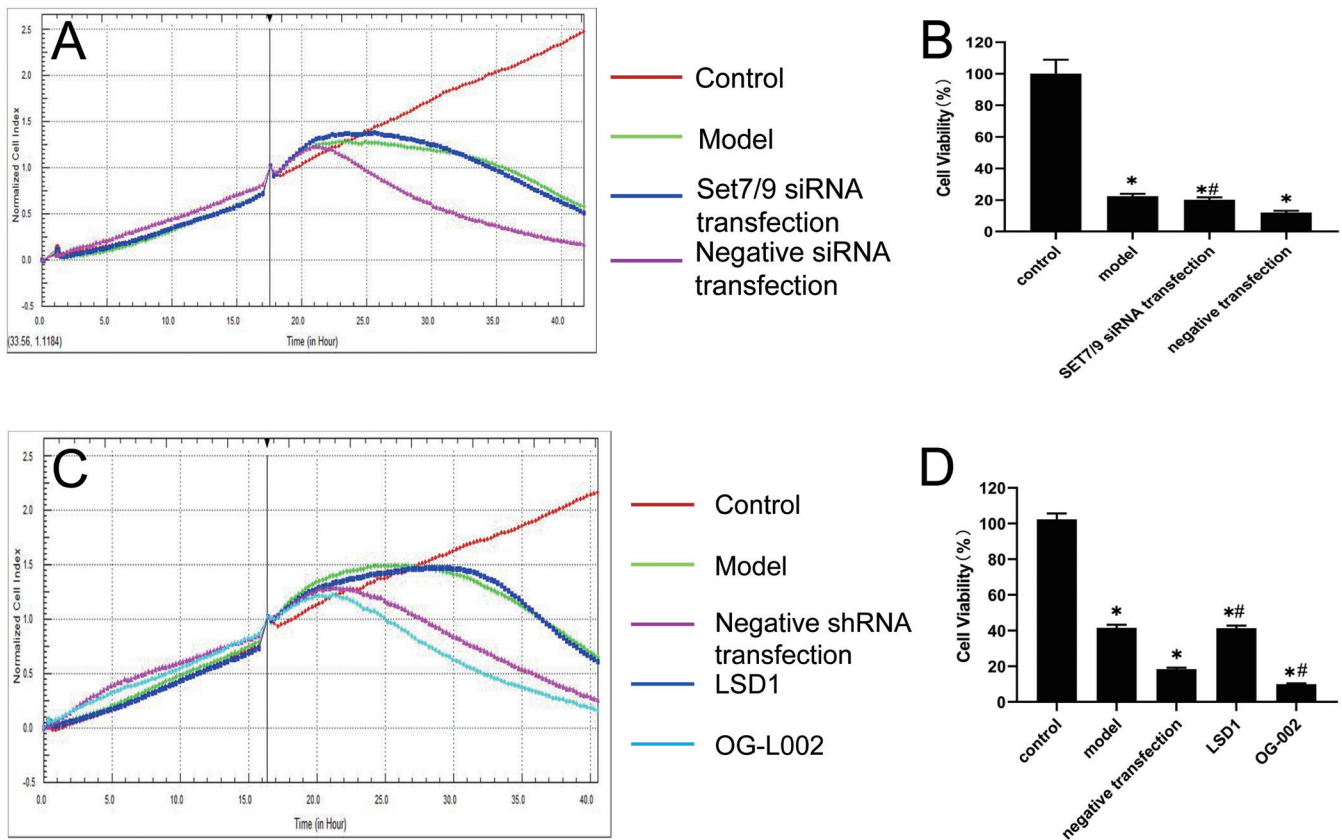


**Fig. 4. Effect of arsenic on growth in L02 hepatocytes.** (A) Real-time cellular analysis was employed to detect the SET7/9 protein knock-down efficiency. Proliferation was measured in control, model and SET7/9 knock-down of L02 cells. (B) The proliferation rate in control, model and SET7/9 knock-down. Data shown are mean±standard deviation of three independent experiments, \* $p < 0.05$  vs. control group; # $p < 0.05$  vs. negative transfection group. (C) Real-time cellular analysis was employed to detect the LSD1 protein knock-down and overexpression efficiency. D: The proliferation rate was measured in control, model and LSD1 knock-down and overexpression LSD1 group. Data shown are mean±standard deviation of three independent experiments, \* $p < 0.05$  vs. control group; # $p < 0.05$  vs. negative transfection group.

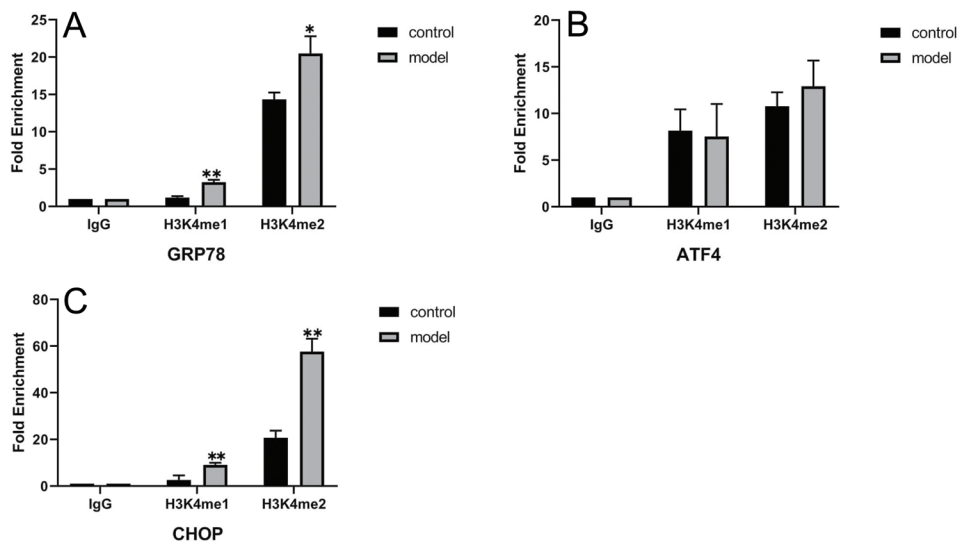


**Fig. 5. Effect of H3K4me1 and H3K4me2 on GRP78, ATF4, and CHOP promoter activity in L02 hepatocytes.** (A) Changes in enrichment of H3K4me1 and H3K4me2 in the GRP78 promoter region. Data shown are mean±standard deviation of three independent experiments; \* $p < 0.05$  vs. control group, \*\* $p < 0.01$  vs. control group. (B) Changes of the enrichment of H3K4me1 and H3K4me2 in the ATF4 promoter region. Data shown are mean±standard deviation of three independent experiments; \* $p < 0.05$  vs. control group, \*\* $p < 0.01$  vs. control group. (C) Changes of the enrichment of H3K4me1 and H3K4me2 in the CHOP promoter region. Data shown are mean±standard deviation of three independent experiments; \* $p < 0.05$  vs. control group, \*\* $p < 0.01$  vs. control group.

Our studies have shown that arsenic can regulate the changes of H3K4me1/me2 level by regulating histone methyltransferase SET7/9 and histone demethyltransferase LSD1 in the process of arsenic-induced hepatocyte apoptosis. Histone H3K4me1/me2 is involved in the activation of ERS-related proteins of GRP78 and CHOP during the process of arsenic-induced hepatocyte apoptosis. This provides a theoretical basis for further elucidating the pathogenesis of arsenic-induced liver injury.

### Acknowledgments

We thank Leng Liang for technical advice in using flow cytometry and microscopy (Basic Medical Science Research Center of Guizhou Medical University). We would like to thank Liu Li for her comments on this manuscript.

### Funding

The present study was supported by the National Natural Science Foundation of China (Grant No. 81100284), Guizhou Science and Technology Cooperation Platform Personnel [2018] (Grant No. 5779-10,5779-19), and Science and Technology Foundation of Guizhou Province (Grant No. ZK [2021]-364)

### Conflict of interest

The authors have no conflict of interests related to this publication.

### Author contributions

Study concept and design (BH), acquisition of data (YY, LT), analysis and interpretation of data (YY, LT), drafting of the manuscript (YY), critical revision of the manuscript for important intellectual content (BH), administrative, technical, or material support, study supervision (BH, QY, RX).

### Data sharing statement

All data are available upon request.

### References

- [1] Kumar R, Mukherji MD, Chakraborty S, Mukherji R. A review on a heavy metal (arsenic) contamination in ground water, soil and translocation in plants. *Indian Journal of Environmental Protection* 2018;38(7):591–600.
- [2] Adeyemi OS, Meyakno E, Akanji MA. Inhibition of Kupffer cell functions modulates arsenic intoxication in Wistar rats. *Gen Physiol Biophys* 2017;36(2):219–227. doi:10.4149/gpb\_2016041.
- [3] Abu El-Saad AM, Al-Kahtani MA, Abdel-Moneim AM. N-acetylcysteine and meso-2,3-dimercaptosuccinic acid alleviate oxidative stress and hepatic dysfunction induced by sodium arsenite in male rats. *Drug Des Devel Ther* 2016;10:3425–3434. doi:10.2147/DDDT.S115339.
- [4] Pompili M, Vichi M, Dinelli E, Erbutto D, Pycha R, Serafini G, *et al*. Arsenic: Association of regional concentrations in drinking water with suicide and natural causes of death in Italy. *Psychiatry Res* 2017;249:311–317. doi:10.1016/j.psychres.2017.01.041.
- [5] El-Bahnasawy MM, Mohammad Ael-H, Morsy TA. Arsenic pesticides and environmental pollution: exposure, poisoning, hazards and recommendations. *J Egypt Soc Parasitol* 2013;43(2):493–508. doi:10.12816/0006406.
- [6] Li C, Li J, Zhang A, Yu C, Xu Y, Xiong X, *et al*. Intervention effects of curcumin on hepatic oxidative stress injury in water arsenic-exposed rats. *Chinese Journal of Endemiology* 2015;34(6):406–410. doi:10.3760/cma.j.issn.2095-4255.2015.06.005.
- [7] Bronkowska M, Łożna K, Figurska-Ciura D, Styczyńska M, Orzeł D, Biernat J, *et al*. Influence of arsenic on selected biochemical blood parameters in

- rats fed diet with different fat and protein content. *Rocz Panstw Zakl Hig* 2015;66(3):233–237.
- [8] Chen L, Zhang A, Yu C, Dong X, Huang X. Arsenic exposure causes human 8-hydroxyguanine DNA glycosidase 1 gene methylation and DNA oxidative damage. *Chinese Journal of Pharmacology and Toxicology* 2014;28(2):216–220. doi:10.3867/j.issn.1000-3002.2014.02.012.
- [9] Santra A, Chowdhury A, Ghatak S, Biswas A, Dhali GK. Arsenic induces apoptosis in mouse liver is mitochondria dependent and is abrogated by N-acetylcysteine. *Toxicol Appl Pharmacol* 2007;220(2):146–155. doi:10.1016/j.taap.2006.12.029.
- [10] Liu S, Li X, Tan C, Liu H, Wu B. Effects of ER stress and PUMA on 5-FU-induced liver cell injury and apoptosis. *Journal of Sun Yat-sen University* 2019;3:364–371. doi:10.13471/j.cnki.j.sun.yat-sen.univ.(med.sci).2019.0052.
- [11] Yang DP, Li J, Huang XX, Zhang AH, Yun H, Xie ZJ. Apoptosis in arsenic poisoning hepatic injury caused by coal burning. *Journal of Military Surgeon in Southwest China* 2005;7(4):1–3. doi:10.3969/j.issn.1672-7193.2005.04.001.
- [12] Xie TT, Zhang AH. Role of p53-mediated mitochondrial apoptotic pathway in arsenic liver injury caused by coal-burning. *Chin J Pharmacol Toxicol* 2014;28(2):210–215. doi:10.3867/j.issn.1000-3002.2014.02.011.
- [13] Liu J, Zhao H, Wang Y, Shao Y, Li J, Xing M. Alterations of antioxidant indexes and inflammatory cytokine expression aggravated hepatocellular apoptosis through mitochondrial and death receptor-dependent pathways in Gallus gallus exposed to arsenic and copper. *Environ Sci Pollut Res Int* 2018;25(16):15462–15473. doi:10.1007/s11356-018-1757-0.
- [14] Zhao H, He Y, Li S, Sun X, Wang Y, Shao Y, *et al*. Subchronic arsenism-induced oxidative stress and inflammation contribute to apoptosis through mitochondrial and death receptor dependent pathways in chicken immune organs. *Oncotarget* 2017;8(25):40327–40344. doi:10.18632/oncotarget.16960.
- [15] Choudhury S, Ghosh S, Mukherjee S, Gupta P, Bhattacharya S, Adhikary A, *et al*. Pomegranate protects against arsenic-induced p53-dependent ROS-mediated inflammation and apoptosis in liver cells. *J Nutr Biochem* 2016;38:25–40. doi:10.1016/j.jnutbio.2016.09.001.
- [16] Wang C, Ning Z, Wan F, Huang R, Chao L, Kang Z, *et al*. Characterization of the cellular effects and mechanism of arsenic trioxide-induced hepatotoxicity in broiler chickens. *Toxicol In Vitro* 2019;61:104629. doi:10.1016/j.tiv.2019.104629.
- [17] Zhang XQ, Xu CF, Yu CH, Chen WX, Li YM. Role of endoplasmic reticulum stress in the pathogenesis of nonalcoholic fatty liver disease. *World J Gastroenterol* 2014;20(7):1768–1776. doi:10.3748/wjg.v20.i7.1768.
- [18] Rasheva VI, Domingos PM. Cellular responses to endoplasmic reticulum stress and apoptosis. *Apoptosis* 2009;14(8):996–1007. doi:10.1007/s10495-009-0341-y.
- [19] Xue QX, Shen X, Tian T, Han B, Xie RJ, He Y, *et al*. Metallothionein decreases the expression of GRP78 and CHOP proteins followed by apoptosis of liver cells in arsenic poisoning rats. *Basic & Clinical Medicine* 2015;35(6):739–743. doi:10.16352/j.issn.1001-6325.2015.06.005.
- [20] Tang L, Xie RJ, Zheng L, Tian T, Yu L, Hu XX, *et al*. Effect of SET7/9-mediated endoplasmic reticulum stress on arsenic-induced hepatocyte apoptosis. *Chinese Journal of Pathophysiology* 2019;35(02):186–189. doi:10.3969/j.issn.1000-4718.2019.02.029.
- [21] Chen J, Guo Y, Zeng W, Huang L, Pang Q, Nie L, *et al*. ER stress triggers MCP-1 expression through SET7/9-induced histone methylation in the kidneys of db/db mice. *Am J Physiol Renal Physiol* 2014;306(8):F916–F925. doi:10.1152/ajprenal.00697.2012.
- [22] Nishioka K, Chuiikov S, Sarma K, Erdjument-Bromage H, Allis CD, Tempst P, *et al*. Set9, a novel histone H3 methyltransferase that facilitates transcription by precluding histone tail modifications required for heterochromatin formation. *Genes Dev* 2002;16(4):479–489. doi:10.1101/gad.967202.
- [23] Tamura R, Doi S, Nakashima A, Sasaki K, Maeda K, Ueno T, *et al*. Inhibition of the H3K4 methyltransferase SET7/9 ameliorates peritoneal fibrosis. *PLoS One* 2018;13(5):e0196844. doi:10.1371/journal.pone.0196844.
- [24] Li ZR, Wang S, Yang L, Yuan XH, Suo FZ, Yu B, *et al*. Experience-based discovery (EBD) of aryl hydrazines as new scaffolds for the development of LSD1/KDM1A inhibitors. *Eur J Med Chem* 2019;166:432–444. doi:10.1016/j.ejmech.2019.01.075.
- [25] Pagrut N, Ganguly S, Tekam S, Pendharkar R, Kumar J. Histological alterations in arsenic induced various organs in rats. *Journal of Entomology and Zoology Studies* 2018;6(3):1428–1429.
- [26] Bali İ, Bilir B, Emir S, Turan F, Yılmaz A, Gökkuş T, Aydın M. The effects of melatonin on liver functions in arsenic-induced liver damage. *Ulus Cerrahi Derg* 2016;32(4):233–237. doi:10.5152/UCD.2015.3224.
- [27] Bambino K, Zhang C, Austin C, Amarasiriwardena C, Arora M, Chu J, *et al*. Inorganic arsenic causes fatty liver and interacts with ethanol to cause alcoholic liver disease in zebrafish. *Dis Model Mech* 2018;11(2):dmm031575. doi:10.1242/dmm.031575.
- [28] Wang LM. Chronic arsenic poisoning caused by long-term taken Niuhuang Ninggong tablet: a report of 2 cases. *Zhongguo Zhong Xi Yi Jie He Za Zhi* 2005;25(3):213.
- [29] Quan NV, Dang Xuan T, Teschke R. Potential hepatotoxins found in herbal medicinal products: A systematic review. *Int J Mol Sci* 2020;21(14):5011. doi:10.3390/ijms21145011.
- [30] Sharma S, Kaur I, Nagpal AK. Assessment of arsenic content in soil, rice grains and groundwater and associated health risks in human population from Ropar wetland, India, and its vicinity. *Environ Sci Pollut Res Int* 2017;24(23):18836–18848. doi:10.1007/s11356-017-9401-y.
- [31] Treleaven J, Meller S, Farmer P, Birchall D, Goldman J, Piller G. Arsenic and ayurveda. *Leuk Lymphoma* 1993;10(4-5):343–345. doi:10.3109/10428199309148558.



- [32] Khandpur S, Malhotra AK, Bhatia V, Gupta S, Sharma VK, Mishra R, *et al*. Chronic arsenic toxicity from Ayurvedic medicines. *Int J Dermatol* 2008;47(6):618–621. doi:10.1111/j.1365-4632.2008.03475.x.
- [33] Danan G, Benichou C. Causality assessment of adverse reactions to drugs—I. A novel method based on the conclusions of international consensus meetings: application to drug-induced liver injuries. *J Clin Epidemiol* 1993;46(11):1323–1330. doi:10.1016/0895-4356(93)90101-6.
- [34] Danan G, Teschke R. RUCAM in drug and herb induced liver injury: The update. *Int J Mol Sci* 2015;17(1):14. doi:10.3390/ijms17010014.
- [35] Teschke R. DILI, HILI, RUCAM algorithm, and AI, the artificial intelligence: Provocative issues, progress, and proposals. *Arch Gastroenterol Res* 2020;1(1):4–11.
- [36] Wu J, Lu T, Cheng ML. Therapeutic effects of the Chinese Medicine Han-Dan-Gan-Le, on arsenic-induced liver injury in Guizhou, China. *Chinese Journal of Endemiology* 2006;25(1):86–89. doi:10.3760/cma.j.issn.1000-4955.2006.01.028.
- [37] He Y, Zhang A, Yang D, Wang J, Wei X, Huang X. Clinical study on treatment to hepatic fibrosis of coal-brunt arsenic with ginkgo leaf. *Journal of Military Surgeon in Southwest China* 2005;7(1):1–3. doi:10.3969/j.issn.1672-7193.2005.01.001.